The durability of the thermal decomposed $IrO_2 - Ta_2O_5$ coated titanium anode in a sulfate solution

Wenting Xu[a,*], Geir Martin Haarberg[a], Frode Seland[a], Svein Sunde[a], Arne Peter Ratvik[b], Susanne Holmin[c], John Gustavsson[c], Åsa Afvander[c], Erik Zimmerman[c], Torjus Åkre[d]

[a] *Department of Materials Science and Engineering, Norwegian University of Science and Technology, Norway*
[b] *SINTEF Industry, Norway*
[c] *Permascand AB, Sweden*
[d] *Glencore Nikkelverk AS, Norway*

Abstract

In this work, series of $IrO_2 - Ta_2O_5$ anodes were investigated. The catalytic activity towards oxygen evolution reaction (OER) of these anodes are determined by calcination temperature, coating loading (coating thickness), pretreatment of titanium substrate and coating method. The difference in OER performance among the anodes are ascribed to the crystallinity of the IrO_2 phase and the phase composition of the coatings. The durability of the anodes were also studied by conducting an accelerated lifetime test (ALT) in acidic 0.9 mol L^{-1} Na_2SO_4 solution at a current density of 5 kA m^{-2}. An anode prepared at a moderate temperature exhibits an excellent lifetime of almost one year although its catalytic activity is not the best. Nevertheless, using the electrostatic spraying method to replace the hand-brush method in the coating preparation can prolong the service life even further and with less amount of coating loading. Moreover, it reveals that the coating loss or combined with titanium substrate passivation results in the eventual deactivation of the anodes during ALT. No critical value of the amount of the residual iridium was found in this work to predict the eventual deactivation before forming the passive oxide film. In addition, the deactivation of the anodes strongly depend on the calcination temperature.

*Corresponding author
Email address: wenting.xu@ntnu.no (Wenting Xu)

Keywords: IrO2-Ta2O5, OER, durability, Catalytic activity, deactivation

1. Introduction

Titanium substrate coated with a conductive layer of metal oxides is well known in the metal electrowinning industry as gas evolving electrode, so-called dimensional stable anode (DSA). The RuO_2-TiO_2 coated titanium is the first commercially successful DSA electrode for chlorine evolution in chlor-alkali electrolysis. Towards the oxygen evolution reaction (OER), this electrode displays better catalytic activity to overcome the kinetic barrier compared to the sluggish kinetics on conventional lead alloy anodes or graphite anode in aqueous electrolysis. It was found that the RuO_2 of rutile structure exhibits excellent OER catalytic activity but it is highly unstable in both acidic and alkaline electrolytes under high anodic potential at high current density, where the RuO_2 (Ru^{4+}) will be oxidized to a soluble RuO_4 (Ru^{8+}) and then dissolve in the solution [1]. Nevertheless, the rutile IrO_2 shows slightly poorer catalytic activity but exhibits much higher stability in the harsh conditions than that of RuO_2 as an anode catalyst for OER. However, IrO_2 is also suffering from a similar problem that Ir^{4+} will be oxidized to Ir^{6+} and dissolve during prolonged OER process [2, 3].

In order to improve the stability of the IrO_2 electrode without losing too much of the catalytic activity, various mixed oxides have been intensively investigated by combining the IrO_2 phase with other non-precious metal oxides, such as SnO_2, Ta_2O_5, TiO_2, SiO_2, Co_3O_4 or Nb_2O_5, to form binary or ternary oxide mixtures [1, 4, 5]. These nonprecious metal oxides can effectively stabilize the IrO_2 during OER, and as a result the catalyst component can be prevented from dissolution for a longer time. Additionally the oxide mixtures offer more active sites than pure IrO_2 oxide since the catalyst component has been dispersed into the stabilizer component. Among those oxide mixtures, the $IrO_2-Ta_2O_5$ is by far the best oxide coating for the OER electrode in acidic electrolyte re-

garding both the catalytic activity and stability, especially in industrial metal electrowinning. Moreover, it has been confirmed that the $IrO_2-Ta_2O_5$ with about 70 wt% iridium gives the best performance in an acidic solution for OER [4, 6, 7]. Although substantial studies have focused on finding an alternative anode to replace $IrO_2-Ta_2O_5$ since iridium is costly, and the service life of this anode is still limited under operation at 40 - 60 °C in sulfate-based corrosive electrolytes and comparably high current density, this type of anode has been used commercially for decades and is still in use [8]. Therefore, further development of both catalytic activity and stability of this type of anode would remain a hot subject in the referred field.

It was reported that the catalytic activity of the $IrO_2-Ta_2O_5$ coated titanium anode is mainly determined by the electrocatalytic active surface area (ECSA), which is strongly depending on the surface morphology of the coating [9, 10]. Apparently this OER performance of the anode would be greatly influenced by the electrode preparation procedure. Industrial anodes are usually produced using the thermal decomposition method, even though other alternative methods such as Sol-Gel, Pechini and electrodeposition have been proposed [11, 12]. The surface morphology of the anodes can be attributed to the preparation parameters (variables) such as the pretreatment of titanium substrate, the coating method, the coating loading (coating loading) and/or the calcination temperature. Nevertheless, the durability of the anode would also be affected by those variables.

Savinell et al. [13] reported that the ECSA of the pure IrO_2 anode is proportional to the loading of the IrO_2 with a range from 0.88 - 2.7 mg cm^{-2}. Later Krýsa and co-workers [14] found that the lifetime of the $IrO_2-Ta_2O_5$ anode (molar ratio Ir : Ta = 6.5 : 3.5) prepared at 450 °C is linearly depending on the iridium content for Ir loading in the range 0.45 to 1.2 mg cm^{-2}. They also reported that the lifetime would depend strongly on the substrate pretreatment with an Ir loading of 0.32-0.39 mg cm^{-2}. However, the anode preparation is not the same in both works which may result in misunderstanding of the real effect of the preparation parameters. In addition, the influence of substrate

pretreatment on lifetime may not relate to the Ir loading [15].

In Hu's work [16], the degradation of the $IrO_2-Ta_2O_5$ anode (molar ratio Ir : Ta = 7 : 3) prepared at 450°C with Ir loading of 0.47 mg cm^{-2} was investigated. It was proposed that the degradation process can be divided into three stages consisting of "active", "stable" and "de-active" About 15 wt% of the coating loss happens rapidly in the first stage followed by a stable dissolution of the coating in a long period as the second stage, and then a peeling off of the coating resulting in the final "de-active" which may be due to the formation of non-conductive TiO_2 layer between Ti and coating interface. The degradation of a similar $IrO_2-Ta_2O_5$ anode but prepared at 500°C was investigated in Xu's work [6]. It concluded that the coating loss in the initial stage is the superficial agglomerates loss by erosion under the attack of intense oxygen evolution, and then the anode suffers at steady state corrosion for a long period. After that the coating begins to loose metallic conductivity, and shows poor electrocatalytic activity, and finally forms a passive oxide layer on the titanium substrate when the Ir content is lower than a critical value.

It seems that the deactivation mechanism might be different while the anode were calcined at different temperatures. However, both deactivation mechanisms are widely accepted today. In addition, the electrolyte temperature for the accelerated lifetime tests in all the above referenced research is different. Thereby, an erroneous understanding might be concluded when combining the results to give the influence of calcination temperature and/or coating loading on the stability of the anode since it has been revealed that the electrolyte temperature has a significant effect in service life tests [8]. The influence of substrate pretreatment on OER performance of the $IrO_2-Ta_2O_5$ anode was also investigated by Yan [17] and Huang [18]. It is manifested that pretreatment procedures affect both catalytic activity and lifetime due to the effect on the surface morphology rather than revealing the intrinsic reason of the influence.

In order to get a better understanding of the deterioration of the $IrO_2-Ta_2O_5$ anode to achieve further improvement of the service life, a series of specific $IrO_2-Ta_2O_5$ anodes prepared at different parameters was studied in the present

Table 1: The details of the preparation for the samples

Sample ID	Pretreatments of Ti Substrate	Coating method	Ir loading[a] (0.3-1.8 mg/cm^2)	Calcination temperature[b] (350-550°C)
A	Sandblasting + Etching	Brush	10 layers	T1
B	Sandblasting + Etching	Brush	10 layers	T2
C	Sandblasting + Etching	Brush	10 layers	T3
D	Sandblasting + Etching	Brush	10 layers	T4
E	Sandblasting + Etching	Spray	11 layers	T3
F	Sandblasting + Etching	Spray	6 layers	T3
G	Sandblasting + Etching	Spray	8 layers	T4
H	Only Etching	Brush	10 layers	T4
I	Only Etching	Brush	5 layers	T4

[a] The order regarding Ir loading amount is 10 layers ¿ 11 layers ¿ 8 layers ¿ 5 layers ¿ 6 layers, and the difference is due to the coating method, it is not possible to present exact Ir loading value due to the commercial consideration. [b] The order regarding calcination temperature is T1 ¡ T2 ¡ T3 ¡T4, it is not possible to present exact temperature due to the commercial consideration.

work. The parameters include calcination temperature, the coating method of brushing and spraying, coating loading (coating loading), and sandblasting as titanium pretreatment. The failure of the referred anodes was also investigated based on implementing all experiments in identical conditions to illustrate the deactivation mechanism regarding those parameters.

2. Experimental methods

2.1. Preparation of the anodes

The $IrO_2-Ta_2O_5$ anodes were prepared on titanium plate by *Permascand AB of Sweden.* Firstly, the titanium substrates (10×10 cm^2) were pretreated by etching after sandblasting or only etching. Subsequently, a thin identical interlayer was prepared on all pretreated titanium substrates to improve the adhesion and impede the formation of the underlying titanium oxide. The precursor solution, which was made in-house and with metal weight ratio Ir : Ta of 8 : 2, then applied upon the interlayer by either manually brushing or

electrostatic-spraying. Then the coated electrodes were dried for 15 minutes at room temperature in order to evaporate the solvent. The desired amount of the coating was achieved by repeating the coating and drying processes. After each time coating, the electrodes were calcined in ambient air for 12 minutes at different temperatures to complete the decomposition of the precursor and to form the metal oxides. The details of the preparation procedure for each sample are described in Table 1.

2.2. Physical characterization

Surface morphology and elemental composition of the anodes were examined using scanning electron microscopy (SEM, *Zeiss Supra*) combined with energy dispersive spectroscopy (EDS). X-ray diffraction (XRD) studies were carried out directly on the surface of samples using Bruker AXS D8Advance with Cu Kα radiation. Those XRD data were collected by varying the 2θ angle from 10° to 80° with an increment of 0.02°. Besides, grazing incident XRD was also employed with grazing incident angle at 3° in order to obtain more phase information of the coating and eliminate the influence from the substrate. The related XRD data were collected with an increment of 0.03° and a measurement time of 4 s per step. The crystalline structure and physical phase of the anodes were calculated based on fitting of XRD patterns. X-ray photoelectron spectroscopy (XPS) measurements were also performed on *Axis Ultra DLD* from *Kratos* in order to analyze the surface chemicals of the anodes. All tested anodes were mounted on top of a carbon tape and placed on the sample stage during the measurements. Spectra and images were acquired with a monochromatic Al Kα X-ray source at energy of 1.48 keV. High-resolution spectra were acquired at 700 μm × 300 μm field of view with analyzer pass energy of 20 eV, and composition spectra were acquired with analyzer pass energy of 80 eV. Binding energies (BEs) of iridium, tantalum and chlorine were referenced to the hydrocarbon C 1 s peak at 285 eV.

2.3. Electrochemical measurements

The electrochemical measurements were performed with a classical three electrode setup with *Gamry REF600* potentiostat. The prepared anodes were used as working electrode, which was fixed in a Teflon sample holder to expose 1 cm^2 of the electrode area. A platinum wire was used as the counter electrode, and a reversible hydrogen electrode (RHE) was used as the reference electrode. All experiments were conducted in 0.9 M H_2SO_4 aqueous electrolyte at 60 °C in a temperature controlled water bath. Preconditioning is necessary as being discussed in our previous work [19], and thus all anodes were run at 100 mV s^{-1} with 200 potential cycles to give satisfactory reproducibility before recording the reported E-I curves. Besides, the electrolyte was de-aerated by argon gas for 30 minutes prior to all measurements.

Cyclic voltammetry (CV) measurements were then recorded between 0.15 V and 1.4 V vs. RHE with sweep rates from 5 to 500 mV s^{-1} in order to determine the ECSA. The ECSA of these anodes is estimated by extrapolating the voltammetric charge q^* to infinitely high sweep rates, i.e. when only the outer charge is probed. The charge is determined by integrating the current vs time curves equivalent to a potential scan between 0.15 and 1.4 V. The total charge q^* can conceptually be split into an inner and an outer charge, according to the following equation [20, 21]:

$$q^* = q_{inner} + q_{outer} \tag{1}$$

where q_{inner} and q_{outer} are the charges related to the "inner" and the "outer" surface, respectively. The inner surface is the less accessible parts of the surface such as pores, cracks, defects and grain boundaries, whereas the outer surface relates to the more accessible parts of the surface to the electrolyte. They also offer an approach to obtain the charge values by extrapolation both at $v = 0(q^*)$ and at $v = \infty(q_{outer})$, where v is the sweep rate.

The electrocatalytic activity of all anodes was investigated by polarization measurements which were conducted from 1.4 V with a sweep rate of 5 mV

min^{-1} to approach steady state. Electrochemical impedance spectroscopy (EIS) was performed at ac sine signal amplitude of 10 mV rms^{-1} from 0.01 Hz to 100 kHz with 10 points per decade. The IR drop was corrected by using the measured electrolyte resistance taken as the high frequency real axis intersection of the electrochemical impedance spectrum. The impedance data were modeled to equivalent circuit Rs (CPE - Rp) with Z-view software.

2.4. Accelerated lifetime tests

By considering that the practical lifetime of this type of anode could be several years, accelerated lifetime tests were carried out to reveal the durability of the anodes as suggested by Comninellis et al. [4]. The lifetime tests were performed in acidic Na_2SO_4 solution (pH = 2) at a current density of 5 kA m^{-2} under galvanostatic condition. The temperature was maintained at 60 °C by using heating elements in the electrolyte. The potential of the electrode was monitored. The electrode was considered to be deactivated when the cell voltage reached 15 V. The lifetime was then recorded as the time until deactivation. X-ray fluorescence (XRF) measurements were carried out on all samples in a different time interval during the test to trace the residual Ir amount in the coatings. For each sample, one more test was performed on the identical twin anode at the same time to control the reproducibility.

3. Results and discussion

3.1. Phase composition and surface morphology

Figure1 depicts the XRD patterns of all samples. The reflections of sample A can be assigned exclusively to the phase of Ti substrate. Since the calcination temperature T1 is too low to acquire complete decomposition and oxidation, amorphous IrO_2 is formed in this coating (sample A). This amorphous IrO_2 might be combined with hydrates as it has been reported in Roginskaya's work [22]. Increasing the calcination temperature up to T2, the coating is still amorphous, but contains a low amount of crystallite IrO_2 of rutile phase so that the

broad IrO_2 peaks can be seen. While calcining the anodes at T3 or T4, the rutile IrO_2 phase is observed with (110), (101), (200) and (211) planes. Apparently the increase of calcination temperature will increase the crystallinity of the IrO_2 phase of the coating. Moreover, there is no Ta_2O_5 related reflection being captured since the Ta_2O_5 phase is amorphous at the current calcination temperature range [19]. Here, it should be added that the coating cannot be fully oxidized in this case, even at T4. This is because only at high temperature (probably higher than 650 °C) the fully decomposition and oxidation can be accomplished [22].

In Fig. 1(b), the IrO_2 related peaks become narrow and have higher intensity with increased calcination temperature. This indicates that the crystallization process of the rutile IrO_2 phase is improved while increasing the calcination temperature from T1 to T4. As a result more crystalline IrO_2 will form and the crystallites will grow larger. Compared to standard PDF card of rutile IrO_2 phase, the observed IrO_2 peaks are slightly shifted to higher 2θ direction with an increase of calcination temperature. This could be because of the formation of $Ir(Ta)O_2$ solid solution which induces lattice strain into the coating layer [19]. As the (110) IrO_2 peak seems to be distributed into 2 or 3 peaks next to each other, it implies that the phase composition of the coating varies with different temperatures.

By comparing samples E to F and/or samples H to I, it can be seen that IrO_2 related peaks become narrower, as shown in Figure 1(c). This means the increase of coating loading will also improve the crystallinity of the IrO_2 phase of the coating. An interesting result is observed in Figure 1(c) where the intensity ratio of (110) IrO_2 to (101) IrO_2 is changed between samples H and I. It seems that the preferred orientation of IrO_2 phase becomes different while applying a different amount of coating loading [19]. Unfortunately, this phenomenon is not observed for samples E and F. However, it might be reasonable since the calcination temperature and the coating method are different for these two groups. Furthermore, using electronic spraying method to replace the hand brushing method will also favor the crystallization of the IrO_2 phase, as shown

in Figure 1(d). No peak shift was found with an increase of coating loading or changing the coating method. This suggests that the calcination temperature dominates the phase composition of the coating in the current case.

Figure 2 shows the surface morphology of all fresh anodes. As can be seen, all surfaces display a typical "mud-crack" structure. Cracks are surrounded by aggregates which are IrO_2 crystallites as we confirmed in a previous study [19]. But the aggregates which are shown in Figure 2 (a) might not be the IrO_2 crystalline structure since the coating of this sample (sample A) is amorphous according to the XRD results above. As a result of the increase of calcination temperature, the cracks become broader and more IrO_2 aggregates form, as can be observed in Figure 2 (a)-(d). Compared to the samples prepared by hand brushing, fewer cracks are formed on the surface of the anodes prepared by electrostatic spraying, as shown in Figure 2 (g).

Moreover, compared to sample C (Figure 2 (c)), sample E (Figure 2 (e)) shows not only fewer cracks on the surface, but also more flat area and more IrO_2 aggregates. This implies that the electrostatic spraying method benefits the crystallization of IrO_2 and resulting in a comparable uniform surface of the coating. This can be ascribed to the more even distribution of precursor solution on the substrate using electrostatic spray compared to hand brushing before calcination. Additionally, the coating surface becomes flatter and has more IrO_2 aggregates formed with an increase of coating loading, as seen in Figure 2 (e) - (f), and (g) - (i). Besides, sample H shows a flatter surface with long cracks as compared to sample D. This demonstrates that the sandblasting would influence the surface morphology, which is due to the increased roughness of titanium substrate before coating [23].

In order to further reveal the effect of those parameters on the surface morphology of the coating, more refined SEM observations of the anodes were carried out. Figure 3 shows the surface morphology of the anodes, with hand brushed 10 layers coating on the etched titanium after sandblasting, which are calcined at different temperatures. No crystalline IrO_2 aggregates are observed on the surface of sample A but cracks which are the same as the ones in Figure 3

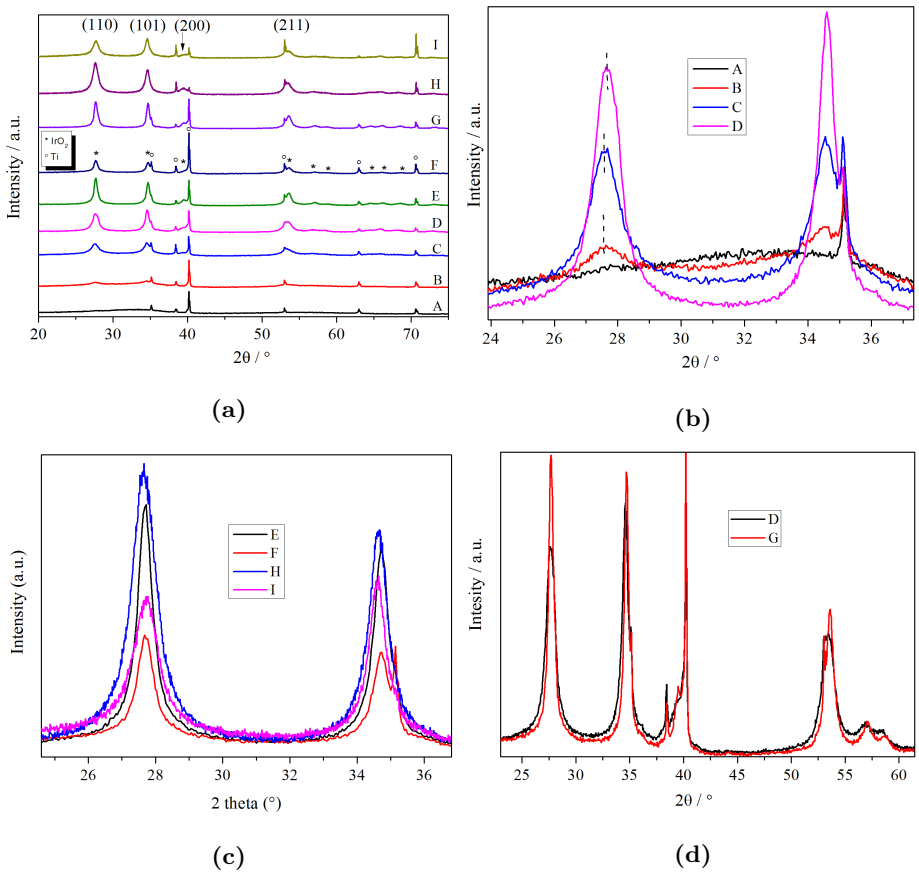

Figure 1: XRD patterns for all anodes, (a) overview XRD patterns for all samples, (b) magnifying the (110) and (101) reflection of the samples A, B, C and D, (c)magnifying the (110) and (101) reflection of the samples E, F, H and I, (d)magnifying the (110) and (101) reflection of the samples D and G

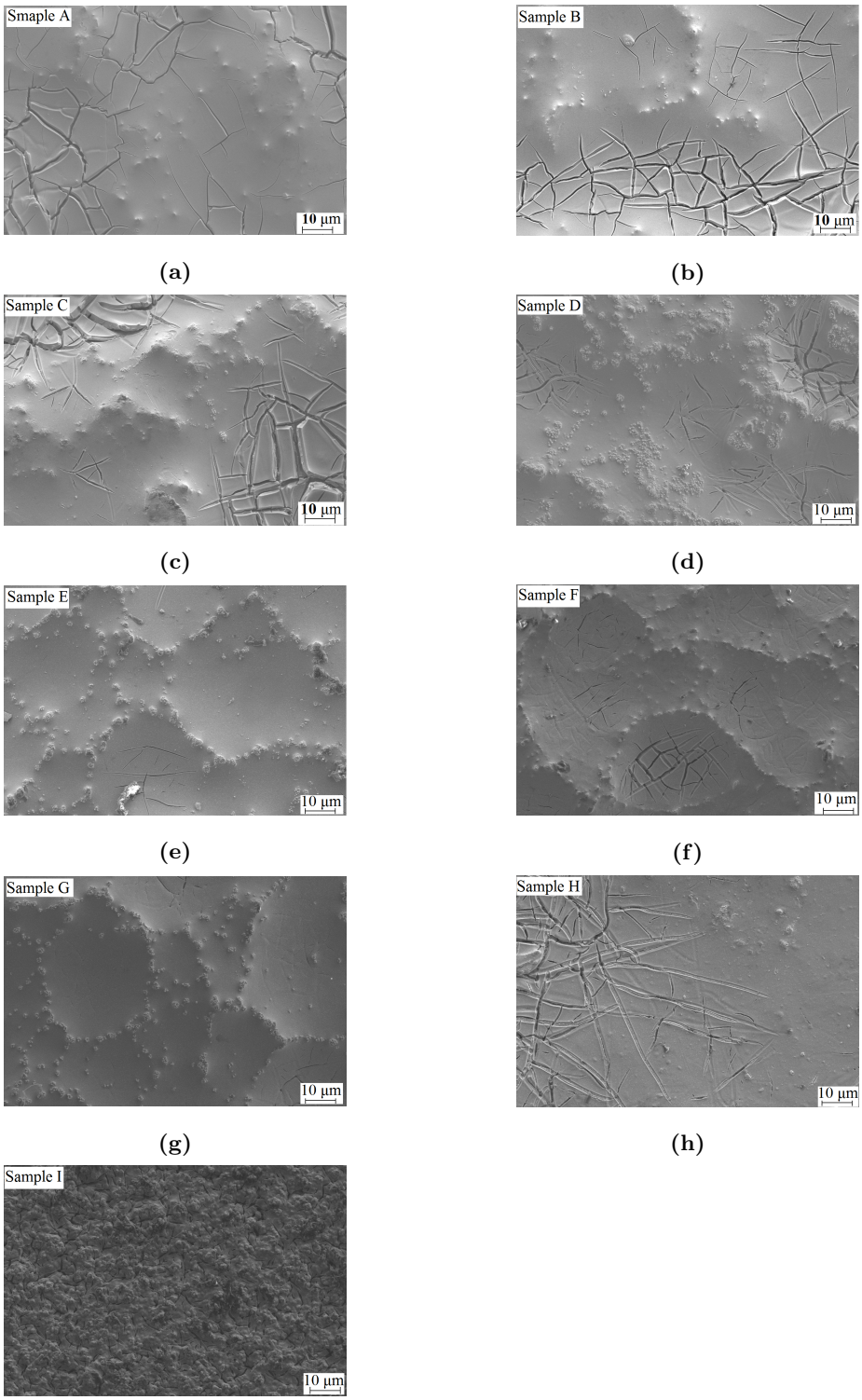

Figure 2: SEM images of all anodes: (a)-(i)sample A-I.

(c) - (d). Needle-shaped IrO_2 aggregates start to form on the coating surface at T2, which then grow larger with further increase of the calcination temperature to T3 and/or T4. Similar needle-shape IrO_2 crystals were also reported in a 70 : 30 mol% $IrO_2-Ta_2O_5$ coating, which exhibited a great OER performance [24]. Some fine IrO_2 crystals start to precipitate inside the cracks at T3 and will grow larger at T4. An interesting phenomenon was observed that some other fine IrO_2 crystals are formed randomly on the top surface of few cracks at T3, as can be seen in the tetragon in Figure 3 (c) and (d). Although these fine IrO_2 crystals are formed with very low density, it might still favor the catalytic activity as all IrO_2 crystals on the coating surface will contribute to the ECSA towards OER as reported in our previous work [19].

Figure 4 shows the surface morphology of the anodes which are prepared by the electrostatic spraying method. The IrO_2 aggregates on the flat area of the surface of these anodes appear with a flower-shaped structure, which grows larger with increased calcination temperature like the ones prepared by hand brushing method. Additionally, those aggregates will also grow larger with an increase of coating loading, as compared in Figure 4 (a) to (c). This is consistent with XRD results. Nevertheless, the IrO_2 crystallites formed inside cracks present similar morphology as the ones in Figure 3. The grain size of these IrO_2 crystallites is almost similar, and independent of calcination temperature. It is notable that very fine IrO_2 particles are formed and distributed homogeneously on the coating surface. The formation of these fine IrO_2 particles with even smaller size has been reported by our group [25], where the dipping coating method was used. Unlike when using the dipping method, these fine IrO_2 particles in this case formed not only on the flat area of the coating surface but all over the surface. This explains the increase of crystallinity degree of IrO_2 phase while using electrostatic spraying method instead of hand brushing method. Figure 5 shows the surface morphology of the samples prepared on the etched titanium substrate and calcined at T4 with different coating loading. The IrO_2 aggregates on the flat area show similar morphology but smaller in grain size as compared to the other hand brushed samples with using sandblast-

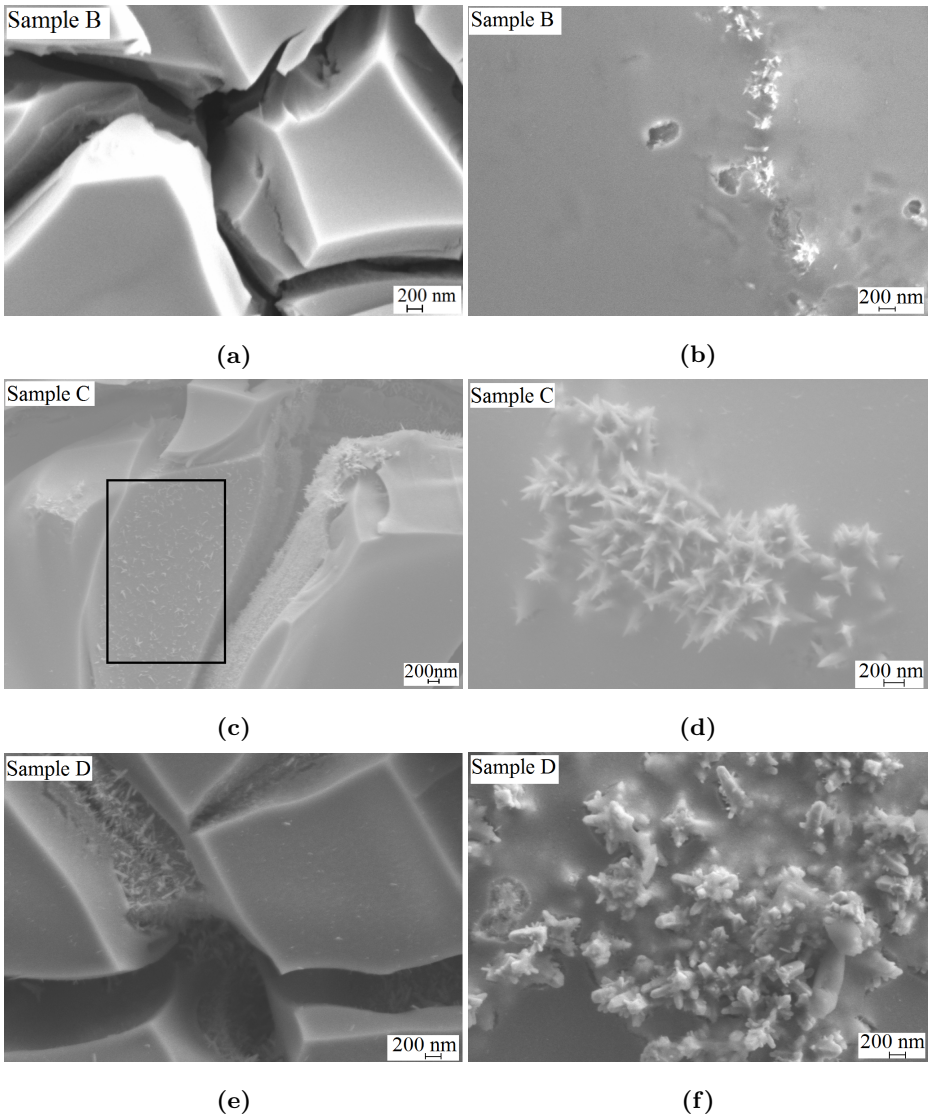

Figure 3: SEM images of the anodes calcined at different temperature (T2 - T4), which are coated by hand brush method on etched titanium substrate followed by sandblasting: (a) & (b)sample B, (c) & (d) sample C , (e) & (f)sample D

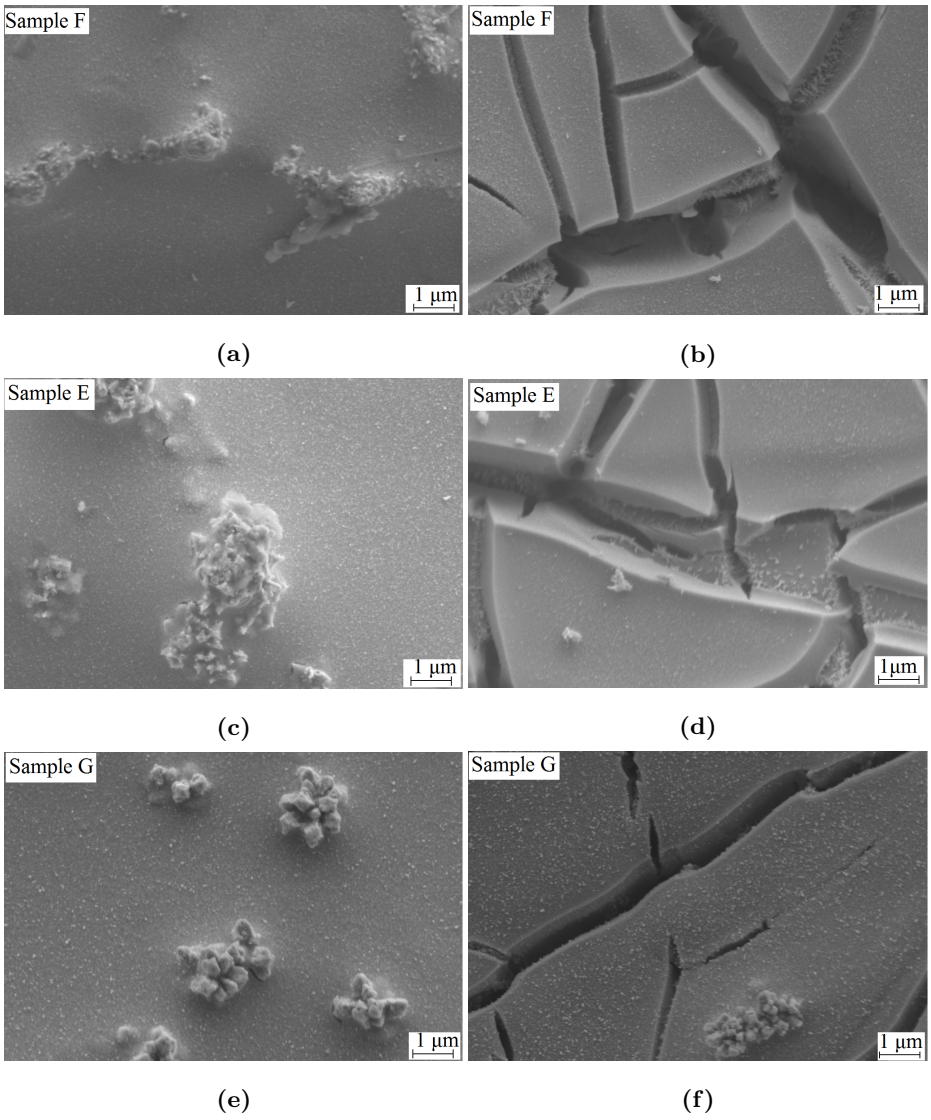

Figure 4: SEM images of the anodes prepared by electrostatic spray method with different coating loading at different calcination temperature: (a) & (b) sample F, (c) & (d) sample E, (e) & (f)sample G

ing in titanium pretreatment. Nevertheless, dense IrO_2 aggregates are formed inside cracks. Obviously, the sandblasting affects the surface morphology of the coating which will influence the OER performance.

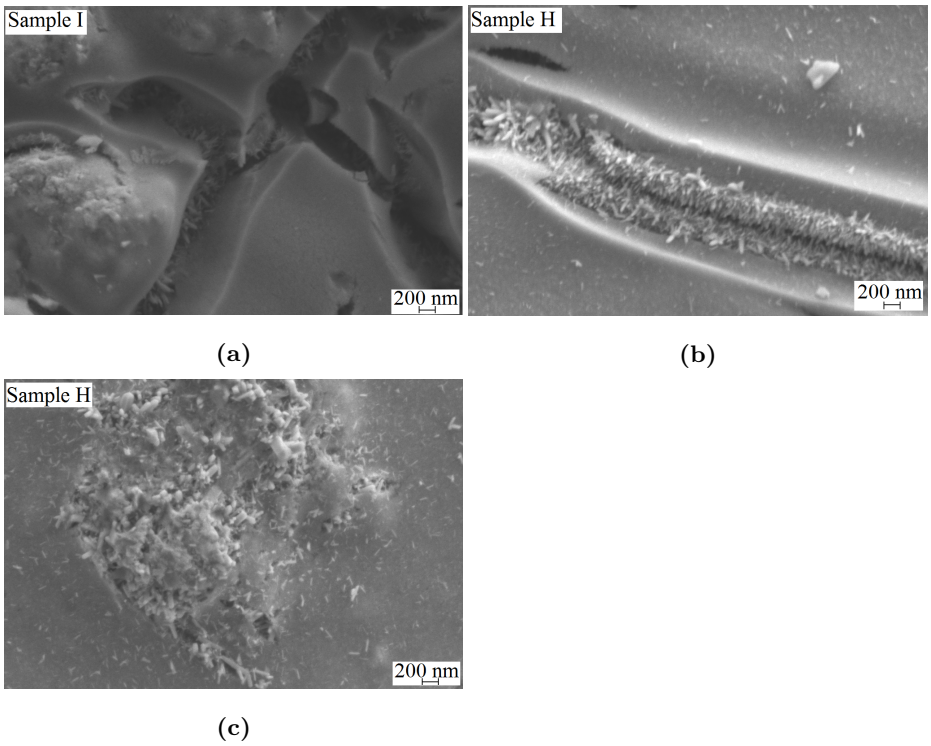

Figure 5: SEM images of the samples prepared on the etched titanium substrate, which are all calcined at T4 with different coating loading: (a) Sample I, (b) & (c) Sample H

3.2. OER performance

The cyclic voltammograms of all samples, recorded between 0.15 and 1.4 V on the reversible hydrogen electrode scale at a potential scan rate of 50 mV s^{-1}, are shown in Figure 6. The observed redox couple between OER and the hydrogen evolution is due to oxidation state transitions of iridium. This is commonly assigned to the Ir^{3+}/Ir^{4+} transitions in this potential range [26]. Unlike the reported redox peaks of pure IrO_2, the referred Ir^{3+}/Ir^{4+} peak on this oxide mixture is very broad. A shift of the referred anodic peak to more negative potentials with increasing calcination temperature from T1 to T4 can be observed in Figure 6. But no shifts are observed while increasing the coating loading. Combining these results to XRD and SEM analysis, the potential for

the Ir^{3+}/Ir^{4+} transitions to take place is calcination temperature dependent, so that this could be attributed to the crystallinity degree of the IrO_2 phase. It is notable that another anodic peak is observed at approximately 0.5 V but only on the amorphous sample which was calcined at T1. This indicates that the IrO_2 formed in the coating of sample A would have more than two oxidation states [27].

The voltammetric charges are calculated by integration of the CV curves as has been described in the experimental section. This charge is considered to be proportional to the number of electroactive sites, which is then representing the ECSA of the anode. As seen in Figure 6 (c) and (d), on the whole, the charge value decreases with an increase of calcination temperature, and/or increases with an increase of coating loading. Therefore, either lowering the calcination temperature or increasing the coating loading can enlarge the ECSA. Additionally, by comparing the voltammetric charge value of sample D to that of sample H, it implies that the sandblasting in the pretreatment of titanium substrate favors increasing the outer part of ECSA. This can be ascribed to the influence of sandblasting on the surface morphology. Moreover, the inner part of ECSA on these two samples is essentially the same since the coating loading is the same. Similar results were elucidated as the influence of substrate pretreatment by Krýsa and co-workers [14].

As an exception in the present case, sample B which was calcined at T2 exhibits a larger ECSA than sample A which was calcined at T1. Regarding that the surface morphology is slightly different between these two samples but the crystallinity of the IrO_2 phase is quite different, as sample A is almost totally amorphous and has more than two oxidation states, it is believed that this amorphous IrOx contributes to fewer active sites than crystalline IrO_2. This amorphous IrOx should be distinguished from the crystalline IrO_2 which has very low crystallinity degree, such as samples A and B in this case.

The catalytic activity towards the OER of all fresh anodes was investigated by anodic polarization measurements. Figure 7 depicts polarization curves for all samples. Regarding the current density values at a potential of 1.5 V, it will

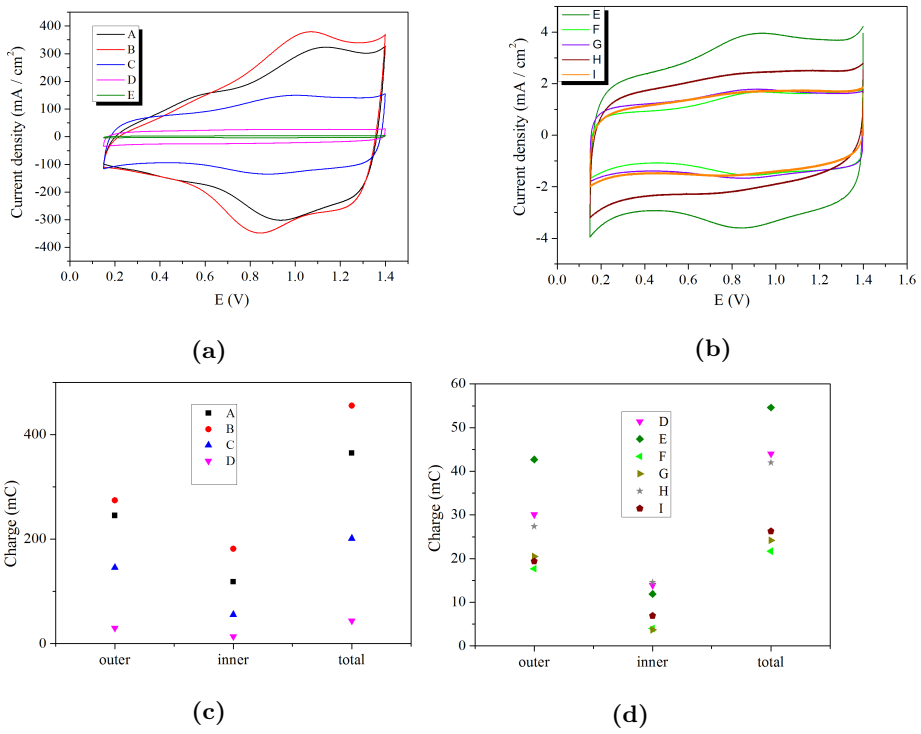

Figure 6: (a) & (b) Cyclic voltammetric curves of the prepared samples, at a scan rate of 50 mV s^{-1}, and (c) & (d) voltammetric charge calculated by integration and extrapolating of CV curves

increase as a result of lowering the calcination temperature or increasing the coating loading, as can be seen in Figure 7 (a). This is in a good agreement with ECSA values. As a common understanding, the catalytic activity is proportional to the ECSA [28]. However, it should be noticed that the catalytic activity is dominated by ECSA but not determined by it. Thereby, sample A shows the best catalytic activity even though the ECSA of sample A is not the largest.

In order to eliminate the influence of ECSA on catalytic activity and to evaluate the catalytic activity of the individual catalyst, the polarization curves are normalized with respect to the outer charge value, as shown in Figure 7 (b). Firstly, it can be seen that the current density at the potential of 1.5 V increases with reduced calcination temperature. Sample A exhibits the best catalytic activity per unit ECSA among all samples. A slight difference between the samples calcined at T4 is observed. This indicates that the catalytic activity per unit ECSA is calcination temperature dependent. Therefore, the catalytic activity of the individual catalyst can be associated with the crystallinity degree of the IrO_2 phase of the coating, which means that the lower the crystallinity degree is the higher the catalytic activity of the catalyst will be. Here, it should be mentioned that the samples B and C are showing similar catalytic activity per unit ECSA since there is only a slight difference on the referred polarization curves. Also, the polarization curves of samples E and F (or samples H and I) are overlapping each other. Similar overlapping of the polarization curves are observed on samples D and G. The overlapping means a similar catalytic activity per unit ESCA. Therefore, neither the increase of the coating loading nor the use of different coating method will affect the catalytic activity of the individual catalyst, which is the same as the effect of the pretreatment of titanium substrate in this case. Evidently, the catalytic activity per unit ECSA of the anodes (or the individual catalyst of the anodes) is only affected by the calcination temperature of the anodes. However, this conclusion is only valid at the low potential range. As can be seen in Figure 7 (b), the polarization curves are bending up and tend to overlap each other at the high potential range. This shows that the catalytic activity per unit ECSA of the anodes in this case is almost the same at the high

potential range.

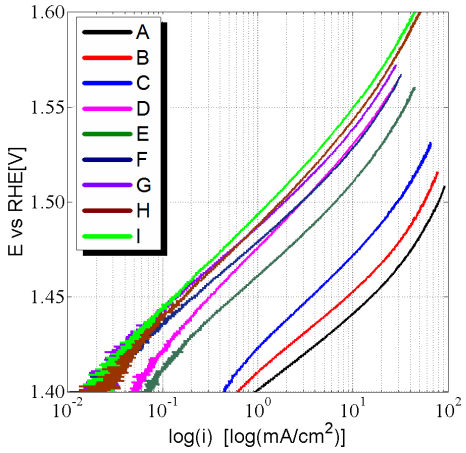

(a)

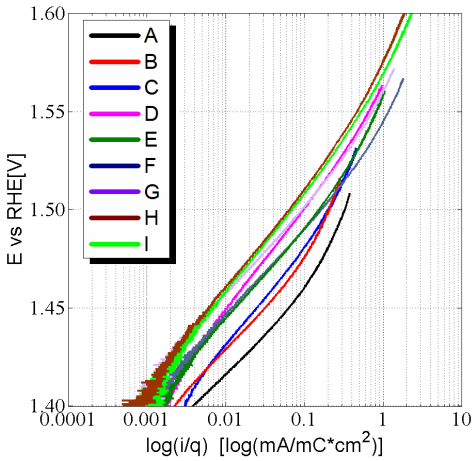

(b)

Figure 7: (a) IR compensated polarization curves of different anodes, at scan rate of 5 mV min^{-1} and (b) Normalized polarization curves on different anodes with respect to outer charge, which gives a measure of the electrocatalytic activity per unit active surface area

It is common that two Tafel slopes would be found on this type of anode [1]. As shown in Table 2, the Tafel slopes (b1) between 40-50 mV dec^{-1} are

Table 2: Tafel slopes of all samples

Tafel slopes ($mV\ dec^{-1}$)	A	B	C	D	E	F	G	H	I
b1	41.5	41.5	45.6	50	48.1	41.7	41.7	50	50
b2					111				

observed at low current density range. The Tafel slope (b2) of 111 mV dec^{-1} was observed on all anodes at high current density range. Both values are a little lower than the average values as reported by Mráz et al. [7]. However a similar trend has been observed, where the Tafel slope b1 increases with an increase of calcination temperature. However, there is no further explanation for this result in the literature.

Usually, the rate determining step (r.d.s.) for OER is the further oxidation of intermediates OH∗ at low current density and the primary discharge of water molecules at high current density [8, 29, 1]. Since the strength of the adsorbed intermediates OH∗ would be influenced by the crystallinity degree of the IrO_2 phase, thus the adsorption of OH∗ could be influenced indirectly by the calcination temperature. As well known, low crystallinity degree means the atoms in the crystalline structure are comparably weaker bonded than that with high crystallinity degree. It seems that the low crystallinity degree benefits the adsorption of the intermediate OH∗, which could possibly be referred to the first Tafel slope (b1). Additionally, the primary discharge seems it would not be affected by the crystallinity degree, as might be referred to b2 value. However, OER is a very complicated process so that further kinetics study is necessary in order to get a better understanding of the related OER mechanism based on transient techniques rather than the derived Tafel slopes [30].

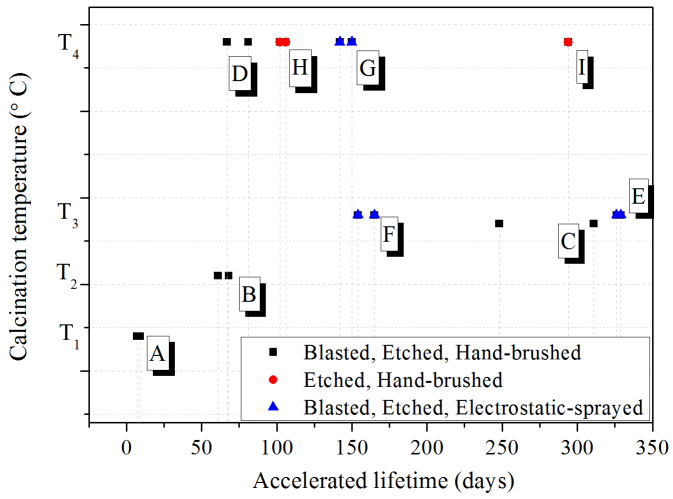

Figure 8: Accelerated lifetime of all prepared anodes (in order to obtain the deviation of the measured lifetime, two identical anodes for each type of sample are employed in the accelerated lifetime tests).

3.3. Accelerated lifetime

The service life, as one of the most significant properties of the anode, was probed by performing an acceleration lifetime test in a laboratory apparatus. As presented in Figure 8, sample E exhibits the best stability among all samples. Although the catalytic activity of sample E is not the best, its lifetime is almost one year under harsh testing condition. Contrary to this, sample A which exhibits the best catalytic activity can only survive approximately one week under the same condition. Obviously, the variation of the accelerated lifetime among the samples is a result of the difference in preparation procedure of the anodes. It can be seen that except for sample I, samples E, C, and F which are calcined at T3 show longer lifetime than the other samples which are calcined at other temperatures. This indicates that T3 is optimal calcination temperature to enhance the anode stability (compared to T1, T2, and T4). Additionally, sample E shows about twice longer lifetime than sample F as it has about 2.5

times more coating loading than the other. This implies that the durability of the anode can be improved by increasing the coating loading. Similar results were reported by Krýsa et al. [14]. However, comparing sample H to sample I, the one with 50% lower loading exhibits three times longer lifetime. Regarding the calcination temperature of these two samples are different to samples E and F, sample I might be an exception due to its different morphology and preferred orientation of IrO_2 phase compared to sample H, while there is only difference on crystallinity degree between sample E and sample F. It should also be mentioned that the lifetime of sample I was recorded up to cell voltage up to 8 volts for a reason, whereas the rest of the anodes are all recorded while the cell voltage reaches 15 volts, so that sample I may have even longer lifetime. Therefore, the effect of coating loading on the lifetime should be associated with the influence of calcination temperature. In another word, the calcination temperature is a more dominant factor for the durability than coating loading. As another result of this conclusion, sample F which has half amount of the coating loading of sample G, exhibits longer lifetime than that.

Furthermore, sample H displays longer lifetime than sample D. This indicates that sandblasting as pretreatment of the titanium substrate will also influence the stability of the anode. The effect has been investigated in detail in previous work, and it was attributed to the shorter distance between the lowest spot of the outer coating surface and the highest spot of the outer substrate while applying sandblasting in titanium pretreatment [23]. Nevertheless, sample E shows better durability than sample C. Regarding the difference in preparation procedure between these two samples, the electrostatic spray method favors improving the durability of the anode.

4. Deactivation mechanism discussion

Martelli and co-workers have summarized the reasons of deactivation of the $IrO_2-Ta_2O_5$ coated titanium anode in laboratory tests [8]. It is including (a) metal base passivation, (b) coating consumption, (c) coating detachment, (d)

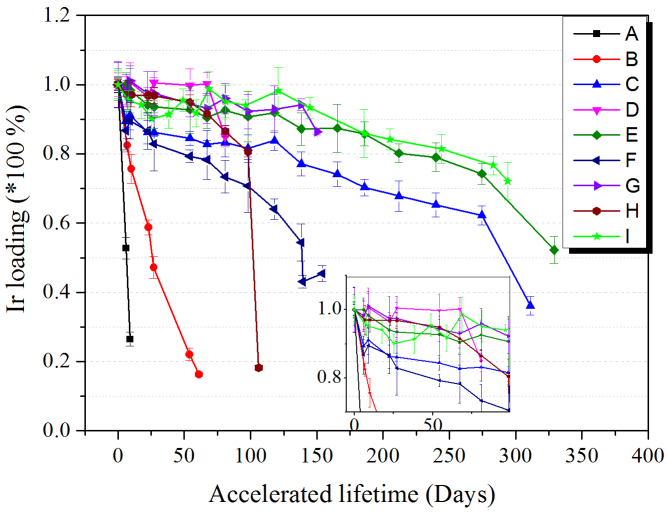

Figure 9: Ir loading versus time during accelerated lifetime test

mechanical damages and (e) mixed mechanism. Considering the durability testing conditions on the samples in present work, the deactivation caused by (d) is unlikely. But it is necessary to get an insight on the intrinsic deactivation mechanism in order to further promote the durability of the anodes.

4.1. Coating loss (coating consumption, coating detachment)

As known, some dissolution of the metal oxide cannot be avoided under OER due to the instability of the oxygen anion in the metal oxide lattice [2]. This dissolution of the metal oxide will definitely result in coating loss. Besides, it should be kept in mind that this dissolution occurs with a very low rate in industrial operation as it is potential dependent [3]. Nevertheless, due to the feature of the porous structure of the coating and the intense gas evolution during the ALT, it might induce the detachment of the coating [8]. It should be mentioned that the coating detachment will also happen in industrial operation, but would be combined with impurity deposition or other side reactions on the anode. Figure 9 shows the residual iridium content in the coating versus time

during ALT. It can be seen that the Ir loss of sample A is very fast although this sample exhibits the best catalytic activity towards OER. A similar phenomenon regarding Ir loss rate is found on sample B but with a slightly smaller loss rate which can be derived by the slope of the related curve. According to the three stages of coating loss in deactivation process which was proposed by Hu et al. [16], there is no "active" stage for samples A and B in our case. The coatings of these two samples are quite unstable, and start dissolving in the beginning and dissolve relatively fast all the way until they are deactivated. As a result, approximately 15 - 25 wt% iridium is left in the coating after deactivation.

Nevertheless, it is also difficult to determine the "active" stage on the samples which are calcined at T4. Unlike the samples A and B, these anodes are more stable. The coatings of these anodes dissolve slowly from the beginning and pass a period of so-called "stable" stage with an approximately constant loss rate. According to the derived slope of the curves within the "stable" stage, the Ir loss rate of these anodes is more or less the same. Then these anodes end up suddenly at the threshold cell voltage in a period so-called "de-active" stage (except for sample I). As can be seen in Figure 9, there is a sudden drop of iridium content before deactivation of the anodes. It is surprising that more than 90 wt% iridium of the initial amount remains in the coatings of these anodes before the final "de-active" starts. Thereby, there should be other reason than iridium loss which results in the eventual deactivation. As the exception, the sample I has about 70 wt% iridium left after dissolving constantly for a long time.

Interestingly, an obvious "active" stage was observed on the samples which are calcined at T3. As shown in the insert figure of Figure 9, a comparably fast Ir loss of the referred samples can be found in the first three weeks. The amount of iridium loss in this period varies from 5 - 20 wt% since the coating loading of each sample is different. Excluding the coating loading effect, it is approximately 0.7 - 0.8 g m^{-2} Ir loss in the "active" stage. Then the coating of these anodes dissolves at a stable rate for a very long period until the final "de-active" takes place. The Ir loss rates in the "stable" stage of these anodes

are different. The loss rate of sample C is twice than that of sample E. Sample F shows a similar loss rate as sample E. Obviously, the coatings prepared by electrostatic spraying method can lower the iridium loss rate in the "stable" stage, which is then prolonging the lifetime of the anodes. It should be stressed that the coating loading also plays a role for the lifetime. As a result, sample F shows the shortest lifetime among these three samples. Besides, compared to the loss rate in the same period of the anodes which are prepared at T4, the increase of calcination temperature can improve the stability of the coating to slow down the iridium dissolution in the "stable" stage. Unfortunately, the anodes prepared at T4 are all deactivated earlier than the anodes prepared at T3, except for sample I.

A critical value of the residual iridium amount has been reported by Xu and Scantlebury [6], and Mráz and Krýsa [7], respectively. This value can be used to indicate the timing point when the final "de-active" starts. However, the final "de-active" of the anodes in the present case happen occasionally and start at a different time. Evidently, there is no critical value for the anodes in our case to indicate the occurrence of the last period of deactivation process.

Based on above discussion, the iridium loss process of the coatings is strongly depending on the calcination temperature of the anodes. As concluded previously, the calcination temperature dominates the crystallinity degree of the IrO_2 phase of the coating. Combining this with the results of the coating loss, the low crystallinity of the IrO_2 phase implies low stability of the coating. Xu and co-workers [6] have explained that the coating loss in the "active" stage is the dissolution of superficial agglomerates of the coating surface, which is due to the weakly bonded atoms of the coating surface. In addition, over time more superficial agglomerates would appear and be exposed to the electrolyte. This will lead to further dissolution of the coating under intensive gas evolution. Thereby, the coating loss of the samples which are calcined at T1 and/or T2 is large, and this is because of the weakly bonded atoms since the crystallinity degree of the IrO_2 phase of referred coatings is pretty low. This is also why no "active" stage exists during the deactivation of the anodes which are calcined at

T4 as the higher the crystallinity degree of referred IrO_2 phase is the stronger the bonded atoms are.

In Figure 10, a significant change in the surface morphology is observed on all deactivated anodes. As a result of coating loss, the surface beneath the coating is visible after the deactivation. Comparing the surface morphology of the deactivated anodes to the fresh anodes (as in Figure 2), a dramatic fragmentation of the coating took place on the samples which are prepared at T1 - T3, especially on the samples A, B and F. It seems that the coating is spalling and peeling off during ALT. This generates more cracks on the residual coating of the anodes.

Moreover, it can be found that spalling of the coating of the anodes prepared at T4 is not that intensive. But the peeling off of the coating of those anodes is remarkable as the titanium substrate is seen, which was confirmed by EDS analysis in previous work [**?**]. The appearance of the titanium substrate indicates that the interlayer of the same area is falling off like the coating or with the coating. Nevertheless, the residual coating of these anodes shows similar morphology as the fresh ones. Relating this to the iridium loss of the coatings, it can be elucidated that these anodes are mainly deactivated by a sudden falling off of the coating and the interlayer. Therefore, it is believed that approximately 80 - 85 wt% iridium remains on those anodes after deactivation. Somehow sample H can still withstand the high current density but meanwhile more coating falls off. As a result the iridium loading of sample H drops from 80 wt% to 19 wt% in a week (seen in Figure 9). Besides, the sample I maintains a relatively constant loss rate of iridium for quite a long time.

In view of the above phenomenon, the coating spalling, iridium dissolution and coating detachment are taking place under intensive gas evolution during ALT. These three processes happen simultaneously and result in the coating loss of the anodes. It is possible that the coating spalling and dissolution would happen at the same time. Then the coating peels off layer by layer and/or by falling off as small pieces from the whole coating assuming that the initial surface still exists. Again, the coating loss is dominated by the calcination temperature

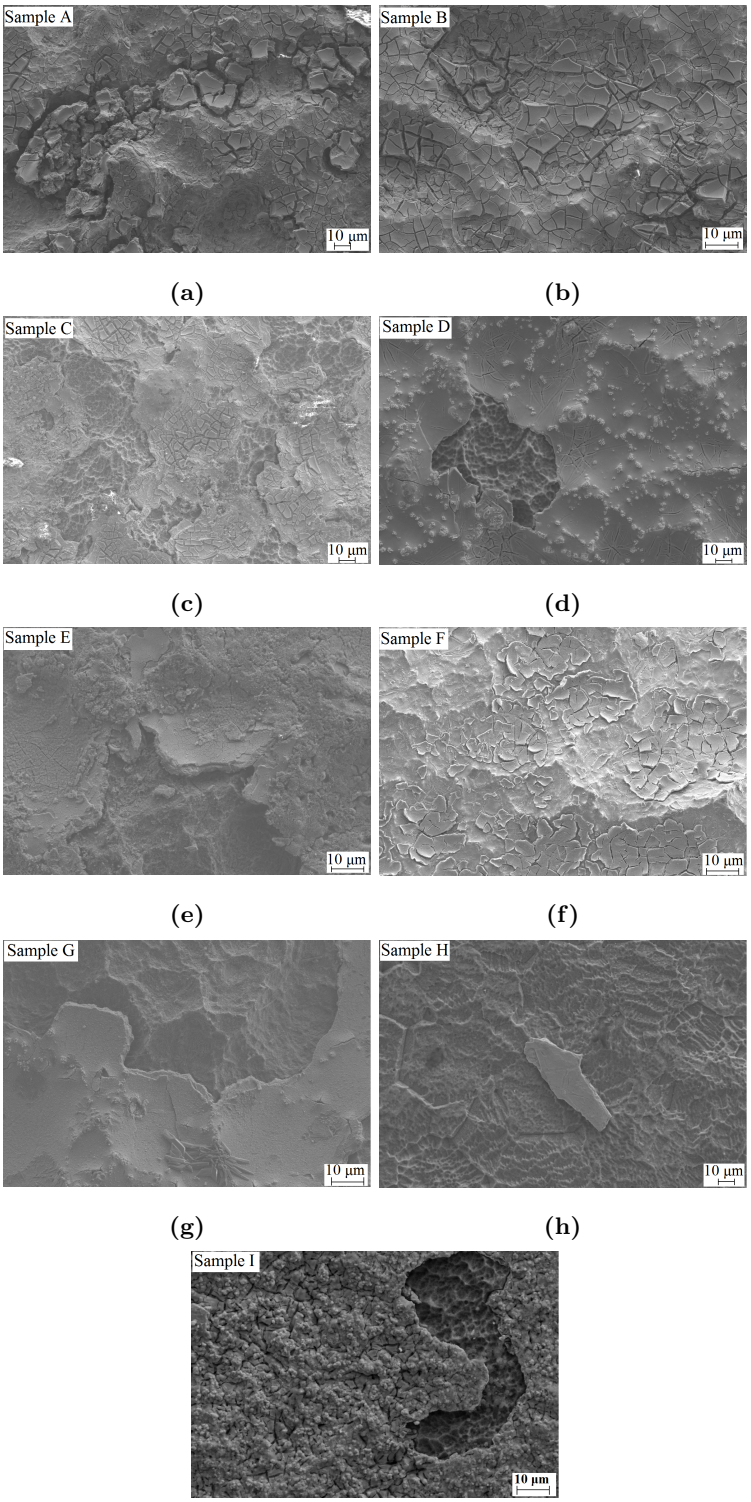

Figure 10: SEM images of all anodes after deactivation: (a) - (i) sample A - I

of the anodes.

4.2. Titanium substrate passivation (oxidation of titanium substrate)

Passivation of the titanium substrate is another distinct reason leading to the deactivation of anodes, especially when the substrate is exposed to the electrolyte [3, 16]. In the last section, as one result of coating loss during deactivation, the titanium substrates of some anodes are exposed after deactivation. This might induce the oxidation of the titanium substrate. It is also possible that the oxidation of the titanium substrate happens firstly and then induces the coating loss as coating detachment [8]. In order to investigate these possibilities, grazing incidence XRD was carried out on all deactivated samples. As depicted in Figure 11, anatase TiO_2 is found but only on the samples which were calcined at T4 (except for sample I). The formation of the anatase TiO_2 will directly lead to the deactivation of the anodes, which usually occurs in the "de-active" stage [6, 16]. That is why quite an amount of iridium is residual on the coating of the referred anodes. It is believed that a fast peeling off of the coating will also take place associated with the titanium oxidation, which results in the change of surface morphology, such as sample H.

The peeling off of the coating was also observed on other anodes which were prepared at T1 - T3, however no anatase TiO_2 is detected on the related deactivated samples. Relating this result to that the interlayer of these anodes is not peeling off, the oxidation of titanium substrate of these anodes is effectively impeded by the interlayer between the coating and the substrate. In another way, the adhesion force between the coating and interlayer of the anodes which are prepared at T4 is stronger, so that the related coating would fall off together with the interlayer compared to the other anodes while in the same ALT. Nevertheless, it is possible that the oxidation of titanium will take place on all anodes regarding the limitation of the detected amount of the XRD. Another possibility would be that the substrate is oxidized to amorphous titanium oxide.

It should be emphasized that sample I, as an exception, has no formation of anatase TiO_2 after deactivation. Since the ALT of the sample I was stopped at

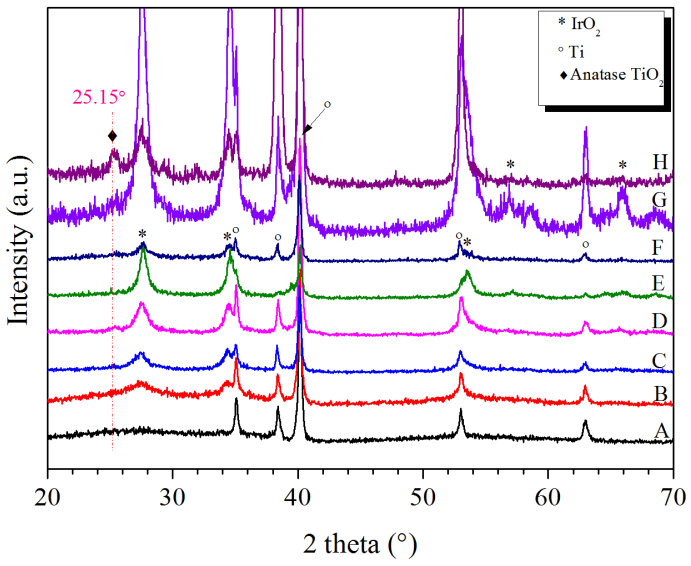

Figure 11: Grazing incidence XRD patterns on deactivated anodes

a cell voltage of 8 V, and coating detachment is also observed on this sample which the coating detachment may occur prior to the formation of anatase TiO_2.

4.3. Calcination temperature dependent deactivation of the anode

Based on above discussion, it can be concluded that the calcination temperature of the anodes has a stronger effect on the deactivation process than the other parameters. Evidently, the coating loss and the passivation of the titanium substrate are both dominated by the calcination temperature of the anodes. For instance, for the anodes prepared at T1 - T2, coating loss is the main reason leading to the eventual deactivation of the anodes. As another example, the formation of anatase TiO_2 results in the eventual deactivation of the anodes which were prepared at T4. In order to further reveal the calcination temperature dependent deactivation of the anodes, the valence states of the coating surface were examined by XPS measurements. The measurements are carried out on the fresh samples A, B, C and D.

The measured spectra of Ir 4f, Ta 4f, and O 1s are shown in Figure 12. The 4f region constitute of two main components is the Ir $4f_{7/2}$ and Ir $4f_{5/2}$, with the spin-orbital splitting of 3.0 eV. Typically, the 4f region of rutile IrO_2 is asymmetric due to its conductive nature [31]. The Ir $4f_{7/2}$ peak of sample D can be fitted with one major asymmetric contribution located at 61.6 eV. This component is attributed to IrO_2 which is in accordance with the literature where the binding energy of Ir $4f_{7/2}$ for rutile IrO_2 powders is typically around 61.6 - 61.9 eV [32, 33, 34, 35]. In addition, there is a minor peak at the high binding energy side (76.3 eV) associated with a satellite contribution. The appearance of a new component at the high binding energy side around 62.2 eV is observed with decreasing of calcination temperature of the anodes. This new component is accompanied with increasing amount of chlorine in the surface as well as increasing amount of hydrated species as $IrCl_3$ and hydrated IrO_2 are reported to be around 62.6 eV and 62.5 eV, respectively, at higher binding energies compared to rutile IrO_2 [33]. The shift towards higher binding energy can be associated with the shift of the XRD peaks of the IrO_2 phase in Figure 1 (b). As a result, Ir $4f_{7/2}$ peak located at 62.4 eV is observed in sample A, which is referred to the amorphous IrO_2. The Ta $4f_{7/2}$ is located at a binding energy of about 26.1 eV for all samples (seen in Figure 12 (b), which is associated with Ta^{5+} species. This value is slightly lower than 26.x to 26.9 typically found for Ta_2O_5 in the literature which can be ascribed to the nature of Ta_2O_5 in this IrO_2 – Ta_2O_5 oxide mixture [36]. These results are in good agreement with XRD results aforementioned. Furthermore, the spectra of the O 1s of the coatings are shown in Figure 12 (c). It is consisting of lattice oxygen (530 eV), hydroxyl groups and/or oxygen defects (531 eV) and adsorbed water (533 eV). Apparently, all these four anodes have these three species in their coatings, but with slight changes in binding energy possibly due to the difference in Ir/Ta ratio. Attempts to separate the oxygen species into two different Ir and Ta-type oxygen species were not attempted. However, it is clear that the coating of the anodes in the current case is not fully oxidized. The formation of hydroxyl and hydrated oxides in the coating of similar anodes has also been

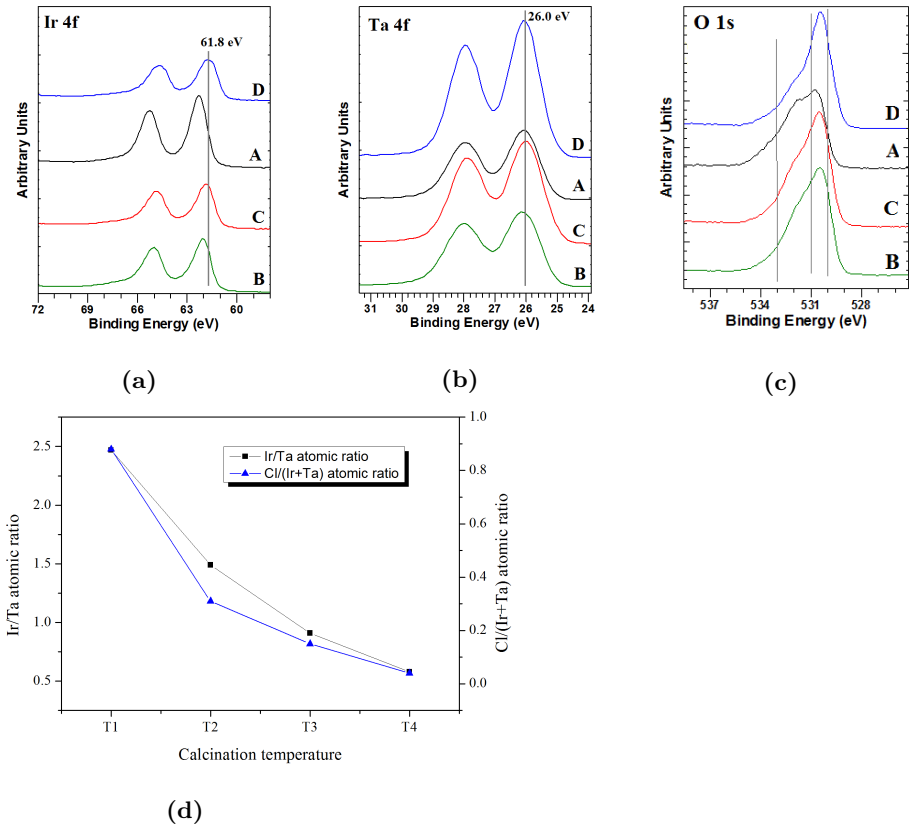

Figure 12: XPS spectra of Ir 4f (a), Ta 4f (b), and O 1s (c) levels for the prepared samples (A, B, C, D), and (d) the related Ir/Ta atomic ratio and Cl/(Ir + Ta) atomic ratio

reported by Augustynski et al. [37]. According to the shape of the O 1s peaks, the amount of each species in the coating of the anodes varies, which can be estimated semi-quantitatively. This results in the difference in crystallinity degree of these anodes. Additionally, as mentioned above chlorine species remains in the coating of the anodes, as illustrated in Figure 12 (d). The residual chlorine of the coating is proportional to the calcination temperature for the anodes. The existence of chlorine indicates that the thermal decomposition of the anodes during calcination is not fully accomplished, not even at T4. Therefore, the coating shows the difference in the rate of coating loss, which is then calcination temperature dependent. The low coating loss rate can be ascribed to the decreased amount of hydrated oxides and/or oxygen defects with increasing calcination temperature. The coating loss rate might also be associated with the residual chlorineof the coating.

Nevertheless, the atomic Ir/Ta ratio is also proportional to the calcination temperature, as can be found in Figure 12 (d). The larger value of the ratio means that more Ir atoms appear on the top surface according to the effective penetration depth of XPS measurement. Owing to this, the sample A which has relatively more Ir atom on the top surface exhibits the best catalytic activity among the samples.

5. Conclusion

In this work, the $IrO_2-Ta_2O_5$/interlayer/Ti anodes prepared under different conditions are studied. According to the electrochemical performance of these anodes towards OER, the catalytic activity of the anodes can be greatly enhanced by lowering the calcination temperature. Nevertheless, increasing coating loading, applying sandblasting before etching in titanium pretreatment or coating with electrostatic spray method instead of hand brushing method will also improve the catalytic activity of the anodes. This is attributed to the influence of the above variables on the physical properties of the IrO_2 phase of the coating. The properties include the crystallinity, the phase composition,

and the Ir/Ta ratio of the top surface of the coating. As a visualized result, the surface morphology of the anodes differ from each other. However, the anode exhibiting the best catalytic activity shows the poorest durability towards long-term OER. The accelerated lifetime of this anode is about 1/50 of the most stable anode.

Furthermore, it is revealed that the deactivation of these anodes is due to the coating loss and the passivation of titanium substrate. The coating loss is due to dissolution, spalling and peeling off. The coating loss will take place simultaneously with OER going on at a constant current density (5 kA cm^{-2} in this work), but the loss rate of the anodes is different. Over time the titanium substrate will be passivated due to the formation of titanium oxide. It shows that the interlayer can prevent or postpone the passivation of the titanium substrate. Evidently, the passivation of the titanium substrate is significantly influenced by the calcination temperature of the anodes. Therefore, the deactivation of the anodes in this work is summarized as follows:

(i) At low calcination temperature (T1 or T2 in this case), the coating of the anodes formed as amorphous or rutile IrO_2 with very low crystallinity. It is associated with the formation of hydroxyl compounds for the coating. These two anodes deteriorate rapidly under the intensive gas evolution during ALT, so that the accelerated lifetime of these anodes is very short. It shows that these anodes are deactivated due to coating loss.

(ii) At high calcination temperature (T4 in this case), the crystallinity of the anodes is improved and the formation of hydroxyl compounds is reduced. As a result, the rate of coating loss of these anodes becomes slower, so that a prolonged lifetime is obtained on the referred anodes. It shows that these anodes are deactivated due to the formation of anatase TiO_2 on the titanium substrate. The passivation of titanium is of course combined with the coating loss during ALT.

(iii) At moderate temperature (T3 in this case), it is successfully achieved the most stable anode which prolongs the lifetime much further. Moreover, coating with electronic spraying method is beneficial to improve the stability

of the anodes with less coating loading. Too low coating loading will result in deactivation due to coating loss.

Acknowledgments

This work is part of the SUPREME project. Financial support from the Research Council of Norway is greatly appreciated, and co-financed by the following industrial companies: *Glencore Nikkelverk*, *Permascand*, *BOLIDEN Odda* and *Hydro Aluminium*. Permission to publish the results is gratefully acknowledged.

References

[1] N. T. Suen, S. F. Hung, Q. Quan, N. Zhang, Y. J. Xu, H. M. Chen, Electrocatalysis for the oxygen evolution reaction: recent development and future perspectives, Chemical Society Reviews 46 (2) (2017) 337–365. doi:10.1039/c6cs00328a.
URL https://www.ncbi.nlm.nih.gov/pubmed/28083578

[2] T. Binninger, R. Mohamed, K. Waltar, E. Fabbri, P. Levecque, R. Kotz, T. J. Schmidt, Thermodynamic explanation of the universal correlation between oxygen evolution activity and corrosion of oxide catalysts, Sci Rep 5 (2015) 12167. doi:10.1038/srep12167.
URL https://www.ncbi.nlm.nih.gov/pubmed/26178185

[3] F. Beck, Wear mechanisms of anodes, Electrochimica Acta 34 (6) (1989) 811–822. doi:https://doi.org/10.1016/0013-4686(89)87114-2.
URL http://www.sciencedirect.com/science/article/pii/0013468689871142https://www.sciencedirect.com/science/article/pii/0013468689871142?via{%}3Dihub

[4] C. Comninellis, G. P. Vercesi, Characterization of DSA-type oxygen evolving electrodes: Choice of a coating, Journal of Applied Electrochemistry

21 (4) (1991) 335–345. doi:10.1007/BF01020219.
URL https://www.scopus.com/inward/record.uri?eid=2-s2.0-0000070436{&}doi=10.1007{%}2FBF01020219{&}partnerID=40{&}md5=a7fdeb089423094b409fb1a56dfc2198https://link.springer.com/content/pdf/10.1007{%}2FBF01020219.pdf

[5] W. Zhang, E. Ghali, G. Houlachi, Review of oxide coated catalytic titanium anodes performance for metal electrowinning, Hydrometallurgy 169 (2017) 456–467. doi:https://doi.org/10.1016/j.hydromet.2017.02.014.
URL http://www.sciencedirect.com/science/article/pii/S0304386X17301093https://www.sciencedirect.com/science/article/pii/S0304386X17301093?via{%}3Dihub

[6] L. K. Xu, J. D. Scantlebury, A study on the deactivation of an IrO2-Ta2O5 coated titanium anode, Corrosion Science 45 (12) (2003) 2729–2740. doi:https://doi.org/10.1016/S0010-938X(03)00108-2.
URL http://www.sciencedirect.com/science/article/pii/S0010938X03001082https://www.sciencedirect.com/science/article/pii/S0010938X03001082?via{%}3Dihub

[7] R. Mràz, J. Krýsa, Long service life IrO2/Ta2O5 electrodes for electroflotation, Journal of Applied Electrochemistry 24 (12) (1994) 1262–1266. doi:10.1007/BF00249891.
URL https://www.scopus.com/inward/record.uri?eid=2-s2.0-0028743482{&}doi=10.1007{%}2FBF00249891{&}partnerID=40{&}md5=09c77fdb2ddda42301545139ccecb88chttps://link.springer.com/content/pdf/10.1007{%}2FBF00249891.pdf

[8] G. Martelli, R. Ornelas, G. Faita, Deactivation mechanisms of oxygen evolving anodes at high current densities, Electrochimica Acta 39 (11-12) (1994) 1551–1558. doi:10.1016/0013-4686(94)85134-4.
URL http://linkinghub.elsevier.com/retrieve/pii/0013468694851344

[9] R. Otogawa, M. Morimitsu, M. Matsunaga, Effects of microstructure of IrO2-based anodes on electrocatalytic properties, Electrochimica Acta 44 (8-9) (1998) 1509–1513. doi:10.1016/S0013-4686(98)00274-6.
URL http://www.sciencedirect.com/science/article/pii/S0013468698002746

[10] S. Trasatti, Physical electrochemistry of ceramic oxides, Electrochimica Acta 36 (2) (1991) 225–241. doi:10.1016/0013-4686(91)85244-2.

[11] L. Xu, Y. Xin, J. Wang, A comparative study on IrO2-Ta2O5 coated titanium electrodes prepared with different methods, Electrochimica Acta 54 (6) (2009) 1820–1825. doi:10.1016/j.electacta.2008.10.004.
URL https://www.scopus.com/inward/record.uri?eid=2-s2.0-58249142861{&}doi=10.1016{%}2Fj.electacta.2008.10.004{&}partnerID=40{&}md5=8e08ed29a0813dbba49e6be0d0baf179https://ac.els-cdn.com/S0013468608012188/1-s2.0-S0013468608012188-main.pdf?{_}tid=b83e45fc-1162-11e8-abb3-00000aab0f26{&}acdnat=1518597813{_}e9641d489901da1ee1d750aa309dc32b

[12] R. A. Herrada, A. Medel, F. Manríquez, I. Sirés, E. Bustos, Preparation of IrO2-Ta2O5—Ti electrodes by immersion, painting and electrophoretic deposition for the electrochemical removal of hydrocarbons from water, Journal of Hazardous Materials 319 (2016) 102–110. doi:10.1016/j.jhazmat.2016.02.076.
URL https://www.scopus.com/inward/record.uri?eid=2-s2.0-84960153564{&}doi=10.1016{%}2Fj.jhazmat.2016.02.076{&}partnerID=40{&}md5=0ebff9092d4824c392373dfa79fbfebahttps://ac.els-cdn.com/S0304389416302102/1-s2.0-S0304389416302102-main.pdf?{_}tid=aabc9314-1164-11e8-9dc5-00000aacb35f{&}acdnat=1518598649{_}d1176724d4b8a278ef4e0af554e7c4ef

[13] R. F. Savinell, R. L. Zeller, J. Adams, Electrochemically Active Surface Area : Voltammetric Charge Correlations for Ruthenium and Iridium Dioxide Electrodes, Journal of The Electrochemical Society 137 (2) (1990) 489–494. doi:10.1149/1.2086468.

[14] J. Krýsa, R. Kule, Làz, I. Roušar, Effect of coating thickness and surface treatment of titanium on the properties of IrO2-Ta2O5 anodes, Journal of Applied Electrochemistry 26 (10) (1996) 999–1005.
URL https://www.scopus.com/inward/record.uri?eid=2-s2.0-0030263337{&}partnerID=40{&}md5=2ead00318e90350e568d13232bfcfc25https://link.springer.com/content/pdf/10.1007{%}2FBF00242194.pdf

[15] W. Xu, G. M. Haarberg, S. Sunde, F. Seland, A. P. Ratvik, S. Holmin, J. Gustavsson, Å. Afvander, E. Zimmerman, T. Åkre, Sandblasting effect on performance and durability of Ti based IrO2-Ta2O5 anode in acidic solutions, Electrochimica Acta.

[16] J. M. Hu, H. M. Meng, J. Q. Zhang, C. N. Cao, Degradation mechanism of long service life Ti/IrO2-Ta2O5 oxide anodes in sulphuric acid, Corrosion Science 44 (8) (2002) 1655–1668. doi:https://doi.org/10.1016/S0010-938X(01)00165-2.
URL http://www.sciencedirect.com/science/article/pii/S0010938X01001652https://ac.els-cdn.com/S0010938X01001652/1-s2.0-S0010938X01001652-main.pdf?{_}tid=d9b292a2-1297-11e8-8455-00000aacb361{&}acdnat=1518730584{_}cae000f53ff946a9d7f2f0e7c1a493c6

[17] Z. Yan, Y. Zhao, Z. Zhang, G. Li, H. Li, J. Wang, Z. Feng, M. Tang, X. Yuan, R. Zhang, Y. Du, A study on the performance of IrO2-Ta2O5 coated anodes with surface treated Ti substrates, Electrochimica Acta 157 (2015) 345–350. doi:10.1016/j.electacta.2015.01.005.

URL http://www.sciencedirect.com/science/article/pii/S0013468615000067

[18] C. A. Huang, S. W. Yang, C. Z. Chen, F. Y. .Hsu, Electrochemical behavior of IrO2-Ta2O5/Ti anodes prepared with different surface pretreatments of Ti substrate, Surface and Coatings Technology 320 (2017) 270–278. doi:10.1016/j.surfcoat.2017.01.005.
URL http://www.sciencedirect.com/science/article/pii/S0257897217300051

[19] W. Xu, G. M. Haarberg, S. Sunde, F. Seland, A. P. Ratvik, E. Zimmerman, T. Shimamune, J. Gustavsson, T. Åkre, Calcination Temperature Dependent Catalytic Activity and Stability of IrO2-Ta2O5 Anodes for Oxygen Evolution Reaction in Aqueous Sulfate Electrolytes, Journal of The Electrochemical Society 164 (9) (2017) F895–F900. doi:10.1149/2.0061710jes.
URL http://jes.ecsdl.org/content/164/9/F895.full.pdf

[20] L. D. Burke, O. J. Murphy, Cyclic voltammetry as a technique for determining the surface area of RuO2 electrodes, Journal of Electroanalytical Chemistry and Interfacial Electrochemistry 96 (1) (1979) 19–27. doi:https://doi.org/10.1016/S0022-0728(79)80299-5.
URL http://www.sciencedirect.com/science/article/pii/S0022072879802995

[21] S. Ardizzone, G. Fregonara, S. Trasatti, "Inner" and "outer" active surface of RuO2 electrodes, Electrochimica Acta 35 (1) (1990) 263–267. doi:https://doi.org/10.1016/0013-4686(90)85068-X.
URL http://www.sciencedirect.com/science/article/pii/001346869085068X

[22] Y. E. Roginskaya, O. V. Morozova, The role of hydrated oxides in formation and structure of DSA-type oxide electrocatalysts, Electrochimica Acta 40 (7) (1995) 817–822. doi:10.1016/0013-4686(95)00002-V.

URL http://linkinghub.elsevier.com/retrieve/pii/001346869500002V

[23] W. Xu, G. M. Haarberg, S. Sunde, F. Seland, A. P. Ratvik, S. Holmin, J. Gustavsson, Å. Afvander, E. Zimmerman, T. Åkre, Sandblasting effect on performance and durability of Ti based IrO2-Ta2O5 anode in acidic solutions (2018).

[24] G. P. Vercesi, J. Y. Salamin, C. Comninellis, Morphological and microstructural the Ti/IrO2-Ta2O5 electrode: effect of the preparation temperature, Electrochimica Acta 36 (5) (1991) 991–998. doi:https://doi.org/10.1016/0013-4686(91)85306-R.
URL http://www.sciencedirect.com/science/article/pii/001346869185306Rhttps://www.sciencedirect.com/science/article/pii/001346869185306R?via{%}3Dihub

[25] K. Kawaguchia, G. M. Haarberg, M. Morimitsu, Nano-Architecture on the Mud-Cracked Surface of IrO2-Ta2O5 Binary System, ECS transactions 25 (33) (2010) 8.

[26] P. Steegstra, M. Busch, I. Panas, E. Ahlberg, Revisiting the Redox Properties of Hydrous Iridium Oxide Films in the Context of Oxygen Evolution, The Journal of Physical Chemistry C 117 (40) (2013) 20975–20981. doi:10.1021/jp407030r.
URL https://doi.org/10.1021/jp407030rhttps://pubs.acs.org/doi/pdfplus/10.1021/jp407030r

[27] A. Minguzzi, O. Lugaresi, E. Achilli, C. Locatelli, A. Vertova, P. Ghigna, S. Rondinini, Observing the oxidation state turnover in heterogeneous iridium-based water oxidation catalysts, Chemical Science 5 (9). doi:10.1039/c4sc00975d.

[28] X. Liu, R. Ma, Y. Bando, T. Sasaki, A general strategy to layered transition-metal hydroxide nanocones: tuning the composition for high

electrochemical performance, Adv Mater 24 (16) (2012) 2148–2153. doi:10.1002/adma.201104753.
URL https://www.ncbi.nlm.nih.gov/pubmed/22447334

[29] J. M. Hu, J. Q. Zhang, C. N. Cao, Oxygen evolution reaction on IrO2-based DSA® type electrodes: kinetics analysis of Tafel lines and EIS, International Journal of Hydrogen Energy 29 (8) (2004) 791–797. doi:https://doi.org/10.1016/j.ijhydene.2003.09.007.
URL http://www.sciencedirect.com/science/article/pii/S0360319903002465https://www.sciencedirect.com/science/article/pii/S0360319903002465?via{%}3Dihub

[30] T. C. Almeida, M. C. E. Bandeira, R. M. Moreira, O. R. Mattos, Discussion on "Electrochemistry of CO 2 corrosion of mild steel: Effect of CO 2 on iron dissolution reaction" by A. Kahyarian, B. Brown, S. Nesic, [Corros. Sci. 129 (2017) 146–151], Corrosion Science.

[31] G. K. Wertheim, H. J. Guggenheim, Conduction-electron screening in metallic oxides: IrO2, Physical Review B 22 (10) (1980) 4680–4683. doi:10.1103/PhysRevB.22.4680.

[32] V. Pfeifer, T. E. Jones, J. J. Velasco Velez, C. Massue, M. T. Greiner, R. Arrigo, D. Teschner, F. Girgsdies, M. Scherzer, J. Allan, M. Hashagen, G. Weinberg, S. Piccinin, M. Havecker, A. Knop-Gericke, R. Schlogl, The electronic structure of iridium oxide electrodes active in water splitting, Phys Chem Chem Phys 18 (4) (2016) 2292–2296. doi:10.1039/c5cp06997a.
URL https://www.ncbi.nlm.nih.gov/pubmed/26700139

[33] S. J. Freakley, J. Ruiz-Esquius, D. J. Morgan, The X-ray photoelectron spectra of Ir, IrO2 and IrCl3 revisited, Surface and Interface Analysis 49 (8) (2017) 794–799. doi:10.1002/sia.6225.

[34] J. M. Kahk, C. G. Poll, F. E. Oropeza, J. M. Ablett, D. Céolin, J. P. Rueff,

S. Agrestini, Y. Utsumi, K. D. Tsuei, Y. F. Liao, F. Borgatti, G. Panaccione, A. Regoutz, R. G. Egdell, B. J. Morgan, D. O. Scanlon, , D. J. Payne, Understanding the Electronic Structure of IrO2 Using Hard-X-ray Photoelectron Spectroscopy and Density-Functional Theory, Physical Review Letters 112 (11) (2014) 117601. doi:10.1103/PhysRevLett.112.117601. URL https://link.aps.org/doi/10.1103/PhysRevLett.112.117601

[35] M. Peuckert, XPS study on thermally and electrochemically prepared oxidic adlayers on iridium, Surface Science 144 (2) (1984) 451–464. doi:https://doi.org/10.1016/0039-6028(84)90111-0.
URL http://www.sciencedirect.com/science/article/pii/0039602884901110

[36] C. Xu, Y. Qiang, Y. B. Zhu, L. T. Guo, J. D. Shao, Z. X. Fan, Laser Damage Mechanisms of Amorphous Ta2O5Films at 1064, 532 and 355 nm in One-on-One Regime, Chinese Physics Letters 27 (11). doi:10.1088/0256-307x/27/11/114205.

[37] J. Augustynski, M. Koudelka, J. Sanchez, B. E. Conway, ESCA study of the state of iridium and oxygen in electrochemically and thermally formed iridium oxide films, Journal of Electroanalytical Chemistry and Interfacial Electrochemistry 160 (1) (1984) 233–248. doi:https://doi.org/10.1016/S0022-0728(84)80128-X.
URL http://www.sciencedirect.com/science/article/pii/S002207288480128Xhttps://www.sciencedirect.com/science/article/pii/S002207288480128X?via{%}3Dihub